

Article

Selective Hydrogenolysis of Glycerol and Crude Glycerol (a By-Product or Waste Stream from the Biodiesel Industry) to 1,2-Propanediol over B₂O₃ Promoted Cu/Al₂O₃ Catalysts

Malaya R. Nanda ¹, Zhongshun Yuan ¹, Hengfu Shui ² and Chunbao (Charles) Xu ^{1,2,*}

¹ Department of Chemical and Biochemical Engineering, Western University, London, ON N6GA5B9, Canada; nandamalaya9@gmail.com (M.R.N.); zyuan25@uwo.ca (Z.Y.)

² School of Chemistry & Chemical Engineering, Anhui University of Technology, Ma'anshan 243002, China; shuihf@sina.com

* Correspondence: cxu6@uwo.ca; Tel.: +1-519-661-2111 (ext. 86414)

Academic Editor: Keith Hohn

Received: 29 April 2017; Accepted: 23 June 2017; Published: 25 June 2017

Abstract: The performance of boron oxide (B₂O₃)-promoted Cu/Al₂O₃ catalyst in the selective hydrogenolysis of glycerol and crude glycerol (a by-product or waste stream from the biodiesel industry) to produce 1,2-propanediol (1,2-PDO) was investigated. The catalysts were characterized using N₂-adsorption-desorption isotherm, Inductively coupled plasma atomic emission spectroscopy (ICP-AES), X-ray diffraction (XRD), ammonia temperature programmed desorption (NH₃-TPD), thermogravimetric analysis (TGA), temperature programmed reduction (TPR), and transmission electron microscopy (TEM). Incorporation of B₂O₃ to Cu/Al₂O₃ was found to enhance the catalytic activity. At the optimum condition (250 °C, 6 MPa H₂ pressure, 0.1 h⁻¹ WHSV (weight hourly space velocity), and 5Cu-B/Al₂O₃ catalyst), 10 wt% aqueous solution of glycerol was converted into 1,2-PDO at 98 ± 2% glycerol conversion and 98 ± 2% selectivity. The effects of temperature, pressure, boron addition amount, and liquid hourly space velocity were studied. Different grades of glycerol (pharmaceutical, technical, or crude glycerol) were used in the process to investigate the stability and resistance to deactivation of the selected 5Cu-B/Al₂O₃ catalyst.

Keywords: boron oxide; Cu/Al₂O₃; glycerol; crude glycerol; 1,2-propanediol

1. Introduction

Owing to its environmental and sustainability benefits, biodiesel, produced mainly by transesterification of vegetable oils or animal fats, has been regarded as a promising substitute to the fossil-based transportation fuels. The biodiesel industry has, however, generated very large amounts of crude glycerol as its primary by-product or waste stream that needs to be disposed. The current global market of glycerol is likely to be saturated because of its limited utilization in different fields [1]. Therefore, there is an urgent need of finding new applications for glycerol or crude glycerol for the sustainability of the biodiesel industry. Chemical valorization is one of the pathways in which glycerol could be converted to high-value chemicals for various applications, which could burst the demand for glycerol.

In fact, catalytic conversion of glycerol to different value-added chemicals, such as acrolein [2], solketal [3,4], glyceric acids [5,6], and propanediols [7–10], are of great industrial importance. Recently, much attention has been given to valorize glycerol to 1,2-propanediol (1,2-PDO) via catalytic hydrogenolysis [11–16]. 1,2-PDO, a three-carbon diol with a stereogenic centre at the central carbon, is one of the high-value chemicals with wide applications. It is mainly used for manufacturing polyester

resins, liquid detergents, cosmetics, tobacco humectants, flavors and fragrances, personal care products, paints, animal feed, anti-freezing agents, and pharmaceuticals [17,18]. Conventionally, it is produced by hydration of propylene oxide derived from petroleum-based propylene either by chlorohydrin or by hydroperoxide processes [19]. Therefore, the development of an alternative renewable process for the production of 1,2-PDO is highly desired from an environmental point of view.

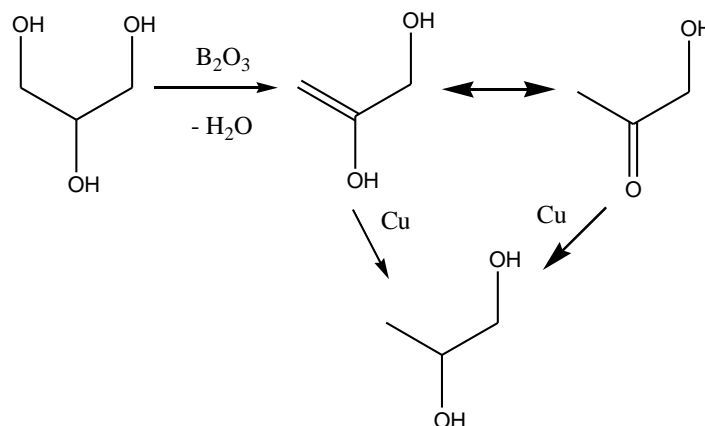
Hydrogenolysis of glycerol to 1,2-PDO over metal-based catalysts, such as Pt, Ru, Ir, Rh, Pd, Ni, and Cu, has been extensively reported in the literature [20–28]. While noble-metal and Ni-based catalysts have demonstrated excellent catalytic activity, these catalysts often promote excessive C–C cleavage, resulting in the formation of degraded, lower-carbon compounds, such as ethylene glycol, ethanol, methanol, and methane [29]. Cu-based catalysts demonstrated to be superior catalysts with excellent catalytic activity [27,28]. Sato, et al. [27], found that copper nanoparticle catalyst prepared from Cu–Al hydrotalcite gave an excellent yield of 1,2-propanediol in the hydrogenolysis of glycerol, achieving 100% conversion of glycerol with 93% 1,2-PDO selectivity at ambient hydrogen pressure through dehydration–hydrogenation via hydroxyacetone (HA). Hydrogenolysis of glycerol to different chemical compounds is given in Scheme 1. The conversion of glycerol to 1,2-PDO involves the selective cleavage of a C–O bond at one of the primary carbon atoms without breaking the C–C bonds of glycerol to eliminate a water molecule, forming acetol as an intermediate compound or side-product, and subsequently absorb a molecule of hydrogen through hydrogenation, thus, requiring a catalyst with dehydration sites which are usually acid sites and hydrogenation sites which usually need a transition metal. Cu is known to be active for C–O bond hydro-dehydration and less active for C–C bond cleavage [30]. The catalytic activity of Cu-based catalyst on different supports such as SiO₂ [31], ZnO [32,33], Al₂O₃ [34,35], Cr₂O₃ [14], zeolite [36], MgO [2], etc., have been investigated. Most of these studies were carried out in a batch reactor, while a continuous-flow process would be more desirable due to the ease of the process scale-up and the potential for commercialization of the process.

Promoters are usually incorporated in a catalyst to enhance its activity and stability. A suitable promoter increases the catalyst surface area and dispersion of the catalyst particles by preventing the agglomeration and sintering of the metals and improves the mechanical strength of the catalyst. Rh, Pd, and silicotungstic acid (H₄SiW₁₂O₄₀) can be effective promoters for Cu-based catalysts for hydrogenolysis of glycerol to 1,2-PDO, however, the use of these expensive promoters in this process would limit its commercialization potential [17,34,37]. The use of inexpensive promoters, such as boric acid, has been reported in Ni/SiO₂ [38] and Cu/SiO₂ [27] catalyst systems with excellent interaction with the metal atoms, resulting a high metal dispersion with a suitable acidity and an outstanding catalytic activity. Hence, it would be interesting to investigate the catalytic behavior of boric acid-doped Cu/Al₂O₃ catalyst for the hydrogenolysis of glycerol.

The selective hydrogenolysis of glycerol to 1,2-PDO has been investigated either in the presence or absence of any solvent [39,40]. For instance, Gandaris et al. demonstrated a novel catalytic conversion process by employing formic acid as both a solvent and a source of hydrogen [21,41]. Chaminand et al. examined the influence of solvent (aqueous and organic) on the hydrogenolysis of glycerol over a Rh/C catalyst in a batch reactor at 180 °C, 80 bar H₂, and for 168 h, and reported a higher glycerol conversion (32%) in the organic solvent (sulfolane) than in water (21%) [24]. As an inexpensive green solvent, water is certainly more desirable than any organic solvents; however, it is challenging to carry out the selective glycerol hydrogenolysis reaction in aqueous medium since water is formed as a by-product during the reaction, which could create a thermodynamic barrier to shift the reaction in the forward direction. Considering the environmental impact of organic solvents and the green/low-cost nature of water, water has been commonly used as a solvent for the selective hydrogenolysis of glycerol to 1,2-PDO [29,42,43].

The use of crude glycerol as a feedstock for the synthesis of propylene glycol is a valuable attempt for the economical production of propylene glycol and the sustainability of the biodiesel industry. However, as mentioned earlier, crude glycerol contains various impurities derived from the biodiesel production processes, including water, sodium or potassium hydroxides, esters, fatty acids, and

alcohols. When crude glycerol is used as a feedstock for the conversion reaction, the impurities would cause operating problems by either deactivating the catalyst or plugging the reactors [11]. There is not much research carried so far on the hydrogenolysis of crude glycerol in a flow reactor. The present work is aimed to investigate on conversion of both pure glycerol and crude glycerol into 1,2-PDO in aqueous medium over inexpensive Cu/Al₂O₃ catalysts promoted by boric acid in a continuous-flow reactor. Therefore, the results of this work will contribute to new knowledge in the literature and open a new window to utilize the crude glycerol for high-value products.



Scheme 1. Hydrogenolysis of glycerol to 1,2-PDO.

The scope of the present work is to study the performance of Cu-based catalysts loaded on highly-dispersed B₂O₃ (which would partially transfer to boric acid in the presence of water) on alumina supports for the glycerol hydrogenolysis reaction. The effects of various process parameters (Cu loading, B addition amount, temperature, H₂ pressure, weight hourly space velocity, purity of the glycerol feedstock, etc.) on the reaction were also investigated. Moreover, the stability of the selected B₂O₃-loaded Cu-based catalyst was tested.

2. Results and Discussion

2.1. Catalyst Characterization

The textural properties of Cu/Al₂O₃ with B₂O₃ promoter measured by Brunauer–Emmett–Teller (BET) theory with N₂ adsorption-desorption isotherms are presented in Table 1. In the Table, an initial improvement in the pore volume and the surface area of the catalyst can be observed by the incorporation of 0.25% B to Cu/Al₂O₃ sample indicating that B₂O₃ helps preventing the agglomeration Cu catalyst. However, the excess of B₂O₃ loading reduced the surface area and pore volume, which could be due to the coverage of the sample surface and blocking of some pores by B₂O₃.

Table 1. Textural properties of the fresh/spent Cu/Al₂O₃ catalysts loaded with various amounts of B₂O₃ determined by N₂ adsorption-desorption.

Catalyst	BET Surface Area (m ² /g)	Total Pore Volume (cc/g)	Pore Diameter (Å)	Amount of Cu (wt%) ¹	Amount of B (wt%) ¹	Amount of Al (wt%) ¹
Al ₂ O ₃	231	0.54	103			
5 Cu/Al ₂ O ₃	152	0.47	100			
5 Cu-0.25B/Al ₂ O ₃	167	0.49	96			
5 Cu-1B/Al ₂ O ₃	131	0.47	99	4.8	0.9	92
5 Cu-3B/Al ₂ O ₃	109	0.32	87			
5 Cu-1B/Al ₂ O ₃ (Spent)	91	0.25	83	4.5	0.2	30

¹ Measured by ICP-AES.

The XRD patterns of the reduced catalyst samples of Cu/Al₂O₃ (containing 5 wt% Cu and 0–3 wt% B) are displayed in Figure 1. In this figure, all the catalysts have similar XRD patterns and the XRD peaks at $2\theta = 36.3, 45.5, 60.6,$ and 66.5 are ascribed to the X-ray diffraction of γ -Al₂O₃ in these catalysts. From Figure 1, one can observe that there is a small peak at 44° in 5Cu/Al₂O₃, typical of copper metal, disappeared after incorporation of B₂O₃. No X-ray diffraction lines of either Cu or B species were detected (although all catalysts contain 5 wt% Cu, above the detection limit of XRD) in 5Cu xB/Al₂O₃ catalysts, suggesting a high dispersion of the corresponding Cu particles in these catalysts.

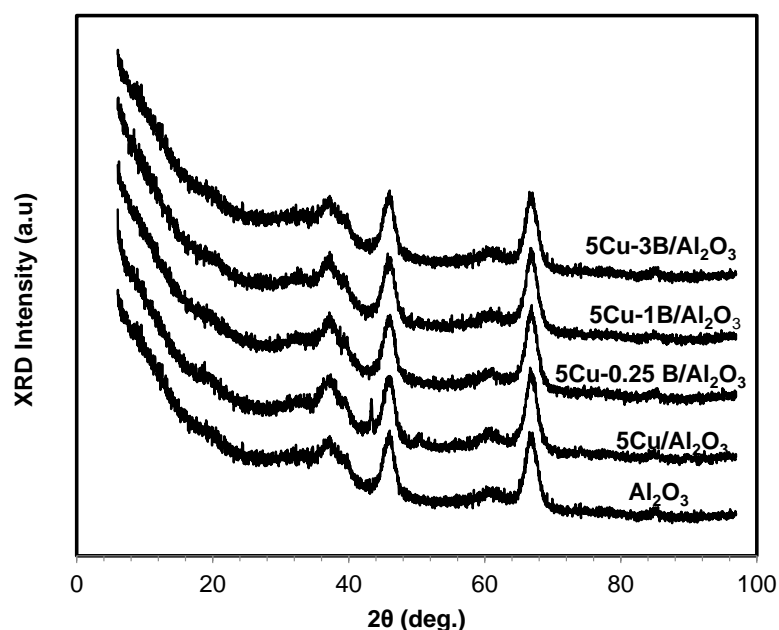


Figure 1. XRD pattern of the fresh Cu/Al₂O₃ catalysts loaded with various amounts of B₂O₃.

The reducibility of the catalysts was investigated using temperature-programmed reduction (TPR). Figure 2 illustrates the hydrogen TPR profiles of all the catalyst samples used in this study. Except 5Cu-0.25B/Al₂O₃, all other samples have a well-resolved single peak in the temperature range of 160–280 °C. The symmetric H₂-TPR profile of the reduction peak indicates the homogeneous nature of the reduced samples and the formation of small, monodispersed metallic Cu particles [34], although in 5Cu-0.25B/Al₂O₃ there exists a main reduction peak and a weak-shoulder peak in the temperature range of 180–220 °C, indicating the presence of two different Cu valence states (Cu⁺¹ and Cu⁰) [44]. In the H₂-TPR profiles (Figure 2), a shift in the reduction peak towards higher temperature with the increase in B content was observed. Similar observations have been reported in the literature where the authors ascribed the peak-shift to the strong interaction between CuO and B₂O₃ [27].

The catalyst acidity has an important role in the bifunctional mechanism (dehydration and hydrogenation) of selective hydrogenolysis of glycerol to 1,2-PDO [20]. Therefore, NH₃-TPD was used to investigate the strength of surface acid sites. The NH₃-TPD profiles of the catalysts are presented in Figure 3. Ammonia is a basic molecule and is adsorbed by the acid sites of the catalyst. The higher is the ammonia desorption temperature, the stronger is acidity of the sites. The larger desorption area, the greater the acid sites. In the figure, a peak between 150 and 250 °C was observed for all the catalysts indicating that weak-intermediate acid sites were present on the catalyst surface [42]. As clearly shown by the NH₃-TPD profiles of the catalysts (presented in Figure 3), the intensity and area of desorption peaks gradually increased, reached maximum for 5Cu-3B/Al₂O₃ with the increase of boron content, proving the increase in acidity of the catalyst surface [38]. Based on the peak areas, the number of acid sites in 5Cu-3B/Al₂O₃ is almost double that of the 5Cu/Al₂O₃ catalyst.

Based on the above characterization results, the roles of addition of B_2O_3 may be summarized here: the addition of B_2O_3 leads to higher reducibility of copper oxides and increased dispersion of Cu particles in the $5Cu-xB/Al_2O_3$ catalysts, which would account for the increased 1,2-PDO selectivity of the catalysts. On the other hand, the addition of B_2O_3 results in increased acidity of the $5Cu-xB/Al_2O_3$ catalysts, which explains the enhanced glycerol conversion, as discussed previously.

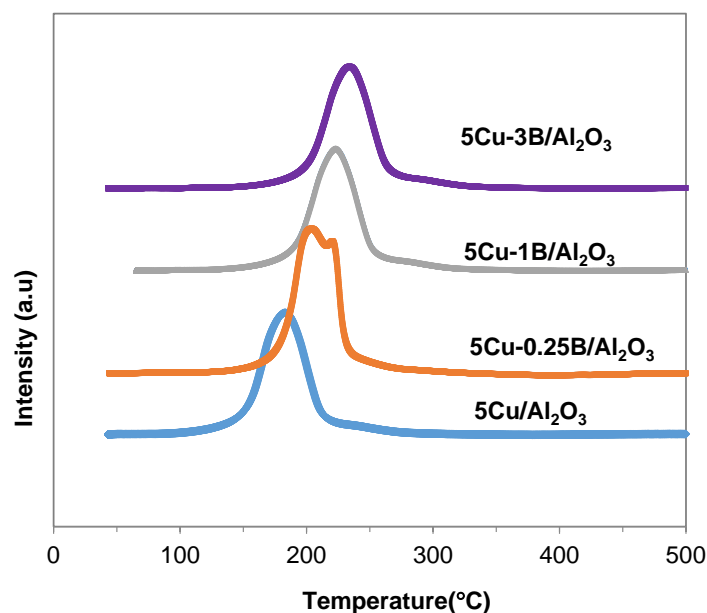


Figure 2. H_2 -TPR profiles of the fresh Cu/Al_2O_3 catalysts loaded with various amounts of B_2O_3 .

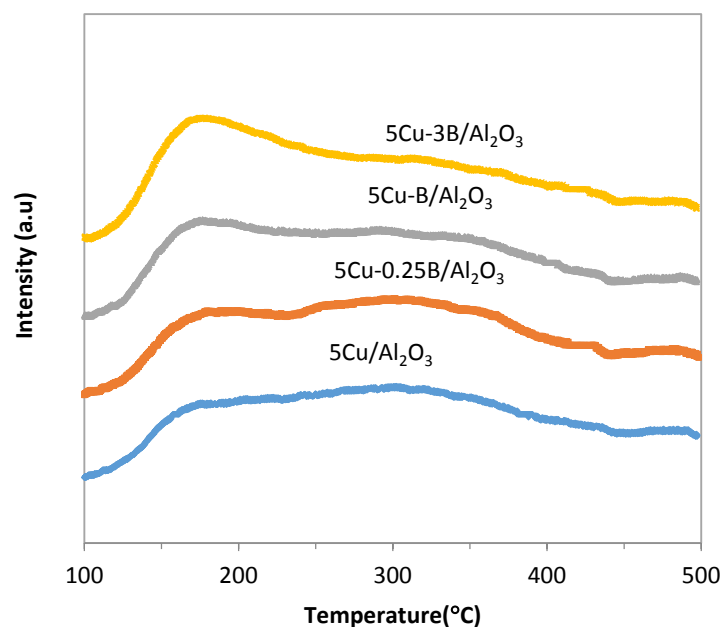


Figure 3. NH_3 -TPD profiles of the catalysts.

2.2. Influence of Process Parameters

2.2.1. Influence of Cu Loading

The effects of Cu loading on the activity of Cu/Al_2O_3 catalysts for glycerol hydrogenolysis were investigated at $230\text{ }^\circ\text{C}$, $5\text{ MPa } H_2$ and 2 h^{-1} WHSV and the results are summarized in Table 2. It can

be seen that with the increase of Cu loading, the glycerol conversion first increased and reached a maximum of 71% at a Cu loading of 5 wt%. This is attributed to the presence of extra active sites produced by the incorporation of Cu which accelerated the reaction process. When further increasing the Cu loading from 5 wt% to 15 wt%, the glycerol conversion and 1,2-PDO selectivity remained almost unchanged, likely due to the reduced dispersion of Cu particles and the blocked pores of the catalyst caused by agglomeration of excess Cu particles in the catalysts with too high Cu loadings. However, the selectivity of 1,2-PDO remains almost unaffected by catalyst loading and was found to be in the range of 85–87% in all the cases. Since 5 wt% loading of Cu metal over alumina demonstrated a promising catalytic performance, it was selected for all the further experiments. From the Table, the main by-products from Cu/Al₂O₃ catalyzed glycerol hydrogenolysis are acetol, ethylene glycol (EG), plus relatively much smaller amounts of compounds denoted as “others” in Table 2.

Table 2. Influence of Cu loading on activity of Cu/Al₂O₃ catalysts for glycerol hydrogenolysis (reaction conditions: 230 °C, 5 MPa H₂ and 2 h⁻¹ WHSV).

Catalyst	Conversion (%)	Selectivity (%)			
		1,2-PDO	EG	Acetol	Others ¹
Al ₂ O ₃	5 ± 1.2	38 ± 0.3	-	57 ± 3.2	5 ± 0.4
1Cu/Al ₂ O ₃	26 ± 2.3	85 ± 3.0	2 ± 0.2	11 ± 0.1	2 ± 0.2
3Cu/Al ₂ O ₃	45 ± 2.0	88 ± 2.0	1 ± 0.1	7 ± 0.6	4 ± 0.6
5Cu/Al ₂ O ₃	71 ± 3.0	87 ± 1.0	3 ± 0.2	6 ± 0.2	2 ± 0.1
10Cu/Al ₂ O ₃	70 ± 2.0	87 ± 2.0	1 ± 0.1	4 ± 0.5	3 ± 0.3
15Cu/Al ₂ O ₃	68 ± 1.0	86 ± 3.0	2 ± 0.2	6 ± 0.4	3 ± 0.4

¹ Others include 1-propanol, 2-propanol, ethanol and methanol.

2.2.2. Influence of B Incorporation

The catalytic effect of B was studied on 5Cu/Al₂O₃ at the reaction conditions of 230 °C, 6 MPa H₂, 2 h⁻¹ (WHSV), and at a hydrogen flow of 100 mL/min, and the results are summarized in Figure 4. The glycerol conversion and 1,2-PDO selectivity for the catalyst 5Cu/Al₂O₃ without B was 73% and 87%, respectively. As B was introduced into the 5Cu/Al₂O₃ catalyst, both catalytic activity and 1,2-PDO selectivity were improved significantly. At these experimental conditions, 5Cu-1B/Al₂O₃ demonstrated the superior performance among other B₂O₃ incorporated catalysts and achieved 80% glycerol conversion with 98% selectivity towards 1,2-PDO. Similar results have been reported by Zhu et al. for B₂O₃-doped Cu/SiO₂ catalysts for the synthesis of propylene glycol [27]. The authors attributed the enhancement in the glycerol conversion to the synergistic effect caused by Cu-B surface interaction which accelerated the surface activity of Cu metal. The improvement in the selectivity towards 1,2-PDO was directly associated with the enhanced hydrogenation activity of Cu towards acetol. A further increase in boron content reduced the glycerol conversion and 1, 2-PDO selectivity, which might be due to the masking effect of boron over the Cu catalyst surface and the pores, as evidenced by the substantial decreases in both BET surface area and total pore volume (Table 1).

There are two possible explanations for the enhancement effects of B₂O₃. First, B₂O₃ can act as a Lewis acid, promoting the dehydration of glycerol to acetol. Secondly, in the calcinations stage, Cu(NO₃)₂ would first decompose to form CuO, then CuO reacts with B₂O₃ to form copper borate, which will convert to well-dispersed nano Cu particles after H₂ reduction. B₂O₃ is usually added to impart thermal stability of a catalyst [45]. Tan et al. used CoB/Al₂O₃ in Fischer-Tropsch synthesis (under conditions comparatively harsher than ours) and reported enhanced thermal stability of the catalyst owing to the presence of boron oxide at the surface sites of the catalyst [45]. However, the mechanism of thermal stabilization of boron incorporated catalysts is not clear. One possible explanation is owing to the strong interaction between Ni and B, and Co and B in Ni-B/SiO₂ and Co-B/MCM-41, respectively, leading to suppression of metal sintering and improvement in the dispersion of active species [38,45]. Yin et al. reported that the incorporation of B₂O₃ to Cu-based

catalysts generated more active sites of Cu in dimethyl oxalate hydrogenation [46]. He et al. [30] proposed that the acidity and electron affinity of B_2O_3 are higher than that of SiO_2 support, which is favorable for the formation of strong interactions between Cu and boron species in Cu-B/ SiO_2 catalysts [47,48]. Thus, in the present study, the stabilizing effect of B_2O_3 could also be due to the strong interaction between Cu and B species which helped retard the aggregation of Cu particles during calcination, reduction, and reaction, as evidenced by H_2 -TPR profiles (Figure 2) clearly indicating a shift in the reduction peak towards higher temperature with an increase in B content.

In addition, as evidenced by the NH_3 -TPD profiles of the non-reduced catalysts (presented in the Figure 3), the addition of B_2O_3 enhanced the acidity of the Cu/ Al_2O_3 catalysts, as similarly reported in the literature [38]. The improved acidity would also play a role in the enhancement of catalytic activities of the catalysts.

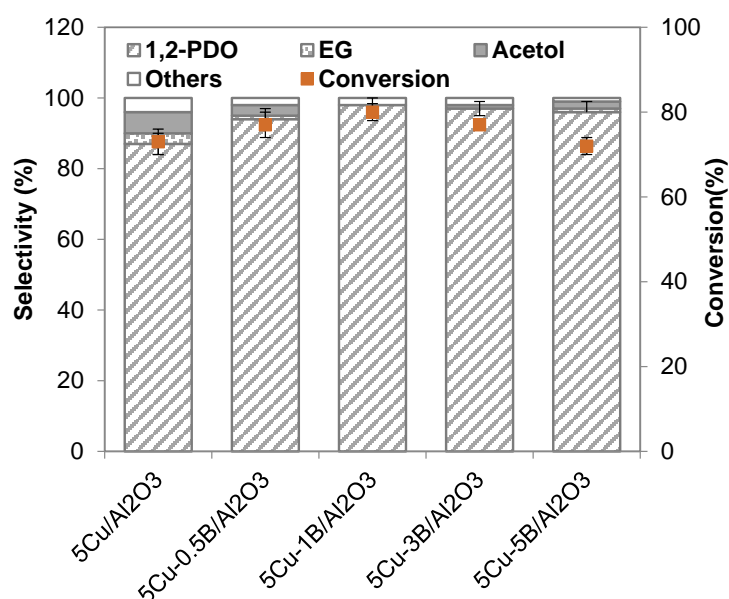


Figure 4. Influence of B loading (0–5 wt%) on 5Cu/ Al_2O_3 on activity of Cu/ Al_2O_3 catalysts for glycerol hydrogenolysis (experimental conditions: 230 °C, 6 MPa H_2 , 10 wt% aq. glycerol, WHSV 0.2 h^{-1}).

2.2.3. Influence of Temperature

The reaction temperature dependence of glycerol hydrogenolysis over 5Cu-B/ Al_2O_3 is illustrated in Figure 5. As expected, the glycerol conversion improved dramatically from 15% (170 °C) to 99% (270 °C) as the temperature elevated. While, an initial insignificant decrease in the 1,2-PDO selectivity from 98% (180 °C) to 96% (250 °C) followed by a remarkable decrease to 85% at 270 °C was observed. It is assumed that the low selectivity at high temperatures is related to the formation of large amounts of undesired by-products, such as the over-hydrogenolysis products 1-propanol, 2-propanol, and the degradation products methanol, ethanol, and ethylene glycol. The selectivity to 1,2-PDO remains high in the moderate range of temperature (200–250 °C), indicating that it is favorable to promote the hydrogenolysis of glycerol to 1,2-PDO in this range of temperatures, as described previously [43].

The reaction mechanisms of glycerol hydrogenolysis to 1,2-propanediol has been reported in the literature [49,50]. Based on the products formed in the present study it is believed that the reaction involves a dehydration and hydrogenation mechanism in which dehydration of glycerol forms acetol which undergoes hydrogenation in the next step to form 1,2-propanediol. The dehydration mainly controlled by the acidity of the catalyst and the hydrogenation occurs on the active metal sites [18]. The other steps involved in the process include the excess hydrogenolysis of 1,2-PDO to form 1-propanol/2-propanol, cleavage of the C–C bond in glycerol to give ethylene glycol and methanol.

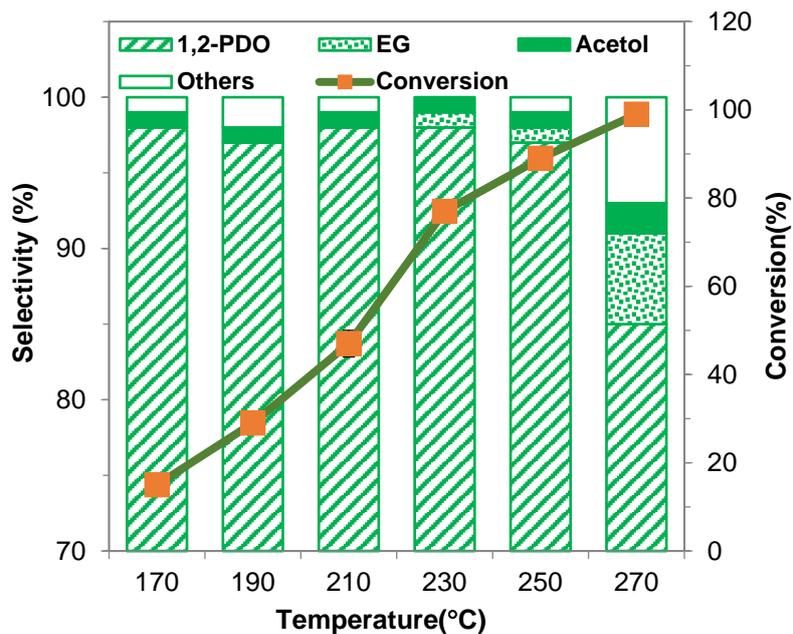


Figure 5. Influence of temperature on the activity of 5Cu-1B/Al₂O₃ catalyst for glycerol hydrogenolysis (5 MPa H₂, 10 wt% aq. glycerol and WHSV 0.2 h⁻¹).

2.2.4. Influence of Hydrogen Pressure

Figure 6 shows effects of hydrogen pressure (2–8 MPa) on the performance of 5Cu-1B/Al₂O₃ catalyst for glycerol hydrogenolysis (240 °C, 10 wt% aq. glycerol and WHSV 0.4 h⁻¹). Generally, both the glycerol conversion and 1,2-PDO selectivity increased by increasing the hydrogen pressure from 2 MPa to 6 MPa, as expected. A further increase in hydrogen pressure did not result in any significant increase in the glycerol conversion and 1,2-PDO selectivity. At 6 MPa H₂, the glycerol conversion and 1,2-PDO selectivity attained 45% and 95%, respectively. The low hydrogen pressure (2 MPa) caused incomplete hydrogenation of acetol to 1,2-PDO.

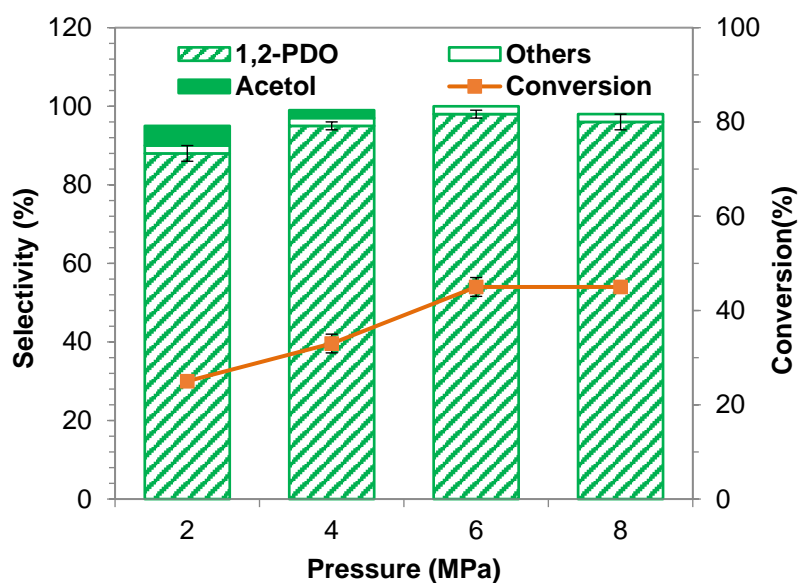


Figure 6. Effects of hydrogen pressure (2–8 MPa) on the performance of 5Cu-1B/Al₂O₃ catalyst for glycerol hydrogenolysis (240 °C, 10 wt% aq. glycerol and WHSV 0.4 h⁻¹).

2.2.5. Influence of Weight Hourly Space Velocity (WHSV)

Effects of WHSV ($0.05\text{--}0.8\text{ h}^{-1}$) on the performance of $5\text{Cu-1B}/\text{Al}_2\text{O}_3$ catalyst for glycerol hydrogenolysis ($250\text{ }^\circ\text{C}$, 6 MPa H_2 , $10\text{ wt\% aq. glycerol}$) were studied by changing the flow rate of the feedstock and the results are shown in Figure 7. It is evident that the glycerol conversion drops with increasing WHSV because of the shortened residence time. However, the selectivity of 1,2-PDO remains almost unchanged ($96\text{--}98\%$) when the WHSV varies between 0.1 and 0.8 h^{-1} , but it was as low as 78% when the WHSV was reduced to 0.05 h^{-1} , which is likely caused by the excessive hydrogenolysis reaction converting 1,2-PDO to ethylene glycol and other lower alcohols like ethanol and methanol at too long a residence time. Hence, to get a good conversion of glycerol with high selectivity to 1,2-PDO, the optimal WHSV is likely 0.1 h^{-1} .

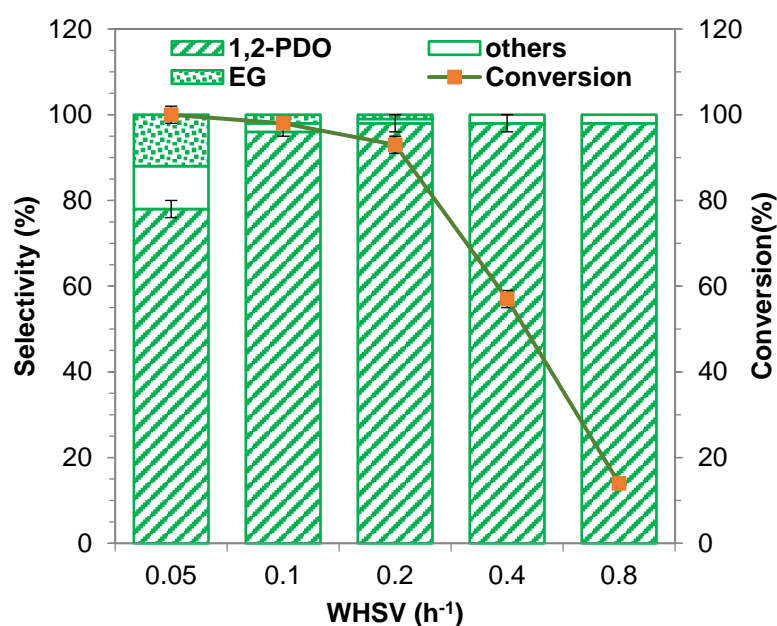


Figure 7. Influence of WHSV ($0.05\text{--}0.8\text{ h}^{-1}$) on the performance of $5\text{Cu-1B}/\text{Al}_2\text{O}_3$ catalyst for glycerol hydrogenolysis ($250\text{ }^\circ\text{C}$, 6 MPa H_2 , $10\text{ wt\% aq. glycerol}$).

2.2.6. Influence of Glycerol Feedstock Purity

One of the objectives of the present work was to evaluate the possibility of using low-grade glycerol for hydrogenolysis to 1,2-PDO. Specifically, crude glycerol (54.7% purity) and technical grade glycerol (91.6% purity) were tested, in comparison to pharmaceutical grade glycerol (99.9% purity). The mass composition of different grades of glycerol used in this work is given in Table 3. It was assumed that the presence of impurities would adversely affect the performance of the catalyst, as discussed previously. For instance, the presence of water would impose a thermodynamic barrier, limiting the reaction. The salt impurities could deactivate the catalyst surface and other organic impurities present in crude glycerol could compete with glycerol in the adsorption process on the catalyst surface, hence, reducing the glycerol conversion and 1,2-PDO selectivity.

Table 3. Composition of different grades of glycerol.

Glycerol Grade	Purity (%)	Water (%)	Ash (%)	MONG ¹ (%)
Pharmaceutical	99.9	0.1	<0.001	N.D
Technical	91.6	4.3	1.4	2.7
Crude	54.7	12.8	7.3	25.2

¹ MONG: matter organic non-glycerol; N.D: not detected.

Figure 8 shows the glycerol conversions and selectivity of different products achieved with different grades of glycerol with 5Cu-1B/Al₂O₃ catalyst at the reaction conditions of 250 °C, 10 wt% aq. solution, 6 MPa, WHSV 0.1 h⁻¹. As expected, reactions performed with technical grade and crude glycerol resulted in substantially reduced glycerol conversion and 1,2-PDO selectivity, which clearly indicates the negative impact of the impurities in the glycerol feedstock on the hydrogenolysis of glycerol due to the deactivation of the catalyst [11].

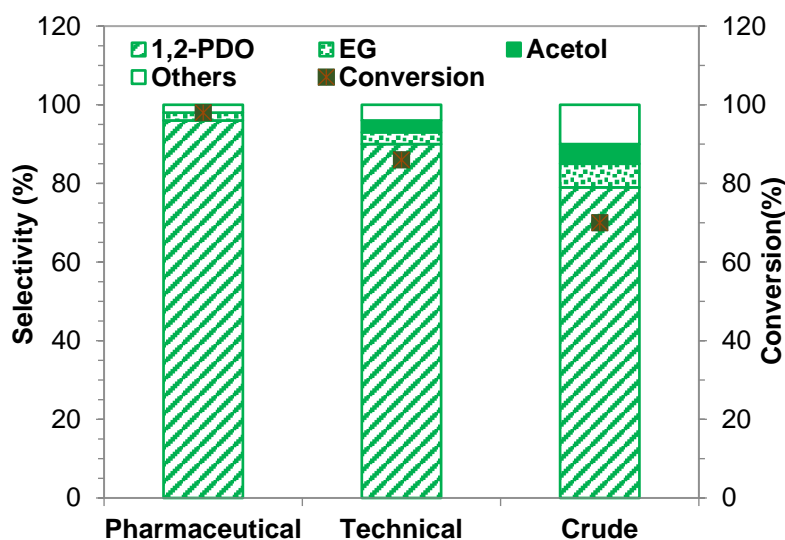


Figure 8. Influence of different grades of glycerol on glycerol conversion and product selectivities with 5Cu-1B/Al₂O₃ catalyst (reaction conditions: 250 °C, 10 wt% aq. glycerol feedstock, 6 MPa, WHSV 0.1 h⁻¹).

2.3. Long-Term Stability and Catalyst Deactivation

The long-term performance of hydrogenolysis of pure glycerol over 5Cu-1B/Al₂O₃ catalyst was tested at 250 °C, 6 MPa H₂ flow, and 0.1 h⁻¹, and the results are given in Figure 9. No sign of any decline in the catalyst activity (>95% glycerol conversion and >97% 1,2-PDO selectivity) was observed up to 60 h, despite the harsh reaction conditions, which suggest the promise of the 5Cu-1B/Al₂O₃ catalyst for industrial applications. After this time, the glycerol conversion gradually decreased. Meanwhile, the product distribution did not show any appreciable change during this period. These results are in good-agreement with those reported in the literature [34]. The list of different products with their selectivity after the first hour of reaction is given in Table 4.

Deactivation of the catalyst was observed after 60 h on stream, as shown in Figure 9. Usually, in a heterogeneous system, the catalyst deactivation occurs due to destruction of the support structure, sintering, coking, fouling, or leaching of the catalyst [51]. Comparing the surface area and the pore volume of the fresh and spent catalyst (Table 1), it is revealed that both the BET surface area and total pore volume for the spent catalyst were reduced, suggesting the destruction of the support, sintering of the Cu metal, or deposition of fouling materials inside the pores of the 5Cu-1B/Al₂O₃ catalyst might occur during the long-term test. To prove this hypothesis, TEM, TGA, and ICP-AES analysis were performed on the fresh and spent (after 70 h on stream) catalysts of 5Cu-1B/Al₂O₃. TEM micrographs of fresh and spent catalyst are illustrated in Figure 10a,b, where the presence of Cu particles was confirmed by Energy Dispersive X-Ray Analysis (EDX). Limited by the magnification of the TEM instrument, however, only clusters of the Cu particles were observable in the fresh and spent catalysts.

Figure 11 shows the TG thermogram of fresh and spent catalysts of 5Cu-1B/Al₂O₃ after 70 h on stream. The TGA measurements were performed at 10 °C/min over a temperature range of 50 °C to 800 °C under a constant flow of air of 20 mL/min. From the TG thermograms of the fresh and spent catalysts, a total of 30 wt% weight loss was observed over the range of 50 °C to 800 °C for the spent

catalyst, compared with only <8 wt% weight loss for the fresh catalyst. This result may evidence the deposition of fouling materials due to polymerization of glycerol on the spent catalyst, which could contribute to the deactivation of the catalyst by blocking the catalyst active sites.

Moreover, the concentration of Cu, B and Al in the fresh and the spent catalyst was measured by ICP-AES and given in Table 1. A negligible change in the concentration of Cu between the fresh and spent catalyst was observed (4.79% to 4.46%) indicating a trivial role of leaching on the catalyst deactivation. However, a significant change in the concentration of B and Al was observed in the spent catalyst indicating the destruction of the support structure in a long run that facilitates the deactivation of the catalyst.

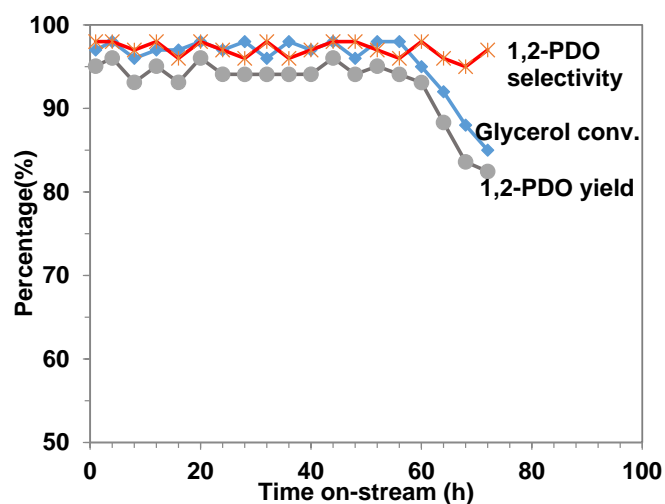


Figure 9. Long term stability of 5Cu-1B/Al₂O₃ catalyst in glycerol hydrogenolysis conducted at 250 °C, 6 MPa H₂ flow and 0.1 h⁻¹.

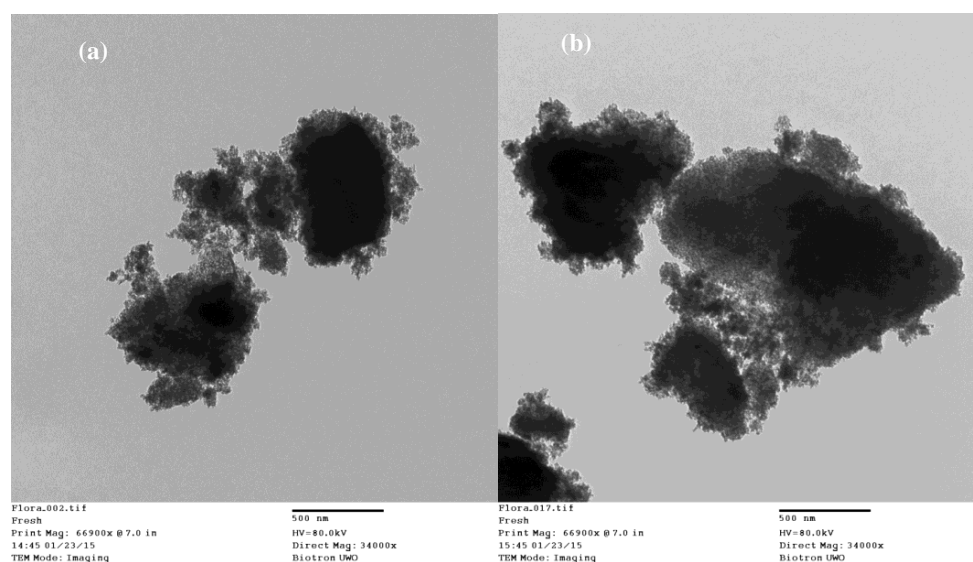


Figure 10. TEM micrographs of fresh (a) and spent catalyst (b) of 5Cu-1B/Al₂O₃ after 70 h on stream.

Table 4. List of different products with their selectivity.

Catalyst	Conversion (%)	Selectivity (%)					
		1,2-PDO	EG	Acetol	1-PrOH	2-PrOH	EtOH
5Cu-1B/Al ₂ O ₃	98 ± 2	98 ± 2.0	0.6 ± 0.03	0.2 ± 0.04	0.6 ± 0.02	0.4 ± 0.04	0.2 ± 0.03

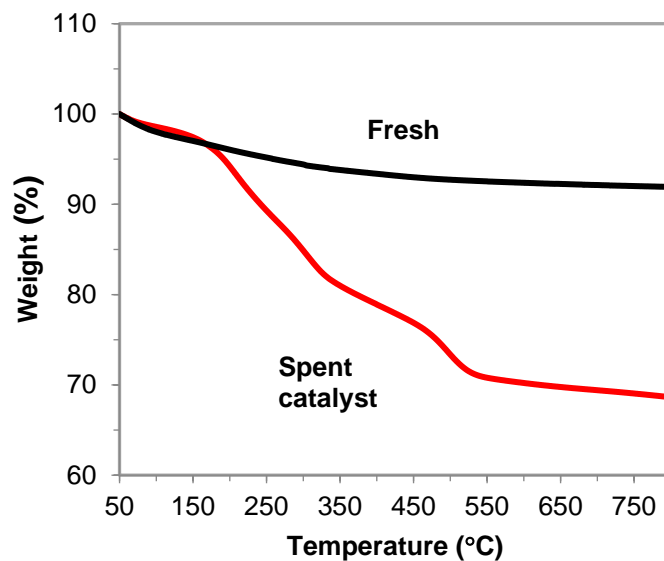


Figure 11. Thermogravimetric analysis of fresh and spent catalyst of 5Cu-1B/Al₂O₃ after 70 h on stream.

3. Materials and Methods

3.1. Materials

Glycerol (99.9%), and methanol (99%), were purchased from Sigma Aldrich Canada (Oakville, ON, Canada) and used as received. Reagent-grade anhydrous ethanol was supplied from Commercial Alcohols Inc (Toronto, ON, Canada). 1,2-propanediol (99.9%), 1,3-propanediol (99.9%), ethylene glycerol (99.9%), acetol (99.8%), *n*-propanol (99.99%), and 1-butanol for GC calibration were also obtained from Sigma Aldrich Canada. Copper nitrate, γ -alumina, and boric acid were purchased from Sigma Aldrich Canada. High purity gases, hydrogen and nitrogen (>99.999%), were obtained from Praxair, Canada Inc (London, ON, Canada).

3.2. Catalyst Preparation

Firstly, a Cu/Al₂O₃ catalyst was prepared by wet impregnation method [34] using a calculated amount of water-soluble metal salt of copper (II) nitrate hydrate [Cu(NO₃)₂·3H₂O] and γ -Al₂O₃ as the support material. The catalyst was then dried at 90 °C for 12 h to form the Cu/Al₂O₃ precursor. The B₂O₃-modified Cu/Al₂O₃ catalysts were prepared by incipient wetness impregnation of the Cu/Al₂O₃ precursor with aqueous solutions containing the desired amount of H₃BO₃. After impregnation, these samples were dried overnight at 90 °C and then calcined at 400 °C for 5 h under a N₂ flow of 20 mL/min at a heating rate of 2 °C/min. The obtained catalysts are designated as xCu-yB/Al₂O₃, where x and y represent the mass loading of copper and boron, respectively.

3.3. Catalyst Characterization

The surface area, total pore volume, and average pore diameter of the selected catalysts were determined by nitrogen isothermal (at −196 °C) adsorption with a Micromeritics ASAP 2010 BET apparatus after degassing the samples at 300 °C for 8 h in vacuum.

The acidity of the catalysts were measured by an ammonia temperature programmed desorption (NH₃-TPD) test using Micromeritics AutoChem II analyzer. Around 0.35 g of the non-reduced calcined catalyst was pretreated in He at 400 °C to remove moisture and other adsorbed gases on the surface for 1 h. After cooling to 100 °C, the catalyst was saturated with pure NH₃ for 30 min, and then purged with He to remove the physisorbed NH₃ for 30 min. The sample was heated to 700 °C at a ramp rate of 5 °C/min and the NH₃ desorbed was detected by a mass spectrometer.

The crystal structures of selected catalysts were examined by powder X-ray diffraction (XRD) with a PANalytical X'Pert Pro diffractometer with Cu K α as the radiation source. Step-scans were taken over the range of 2 θ from 6 to 95 $^\circ$.

Temperature-programmed reduction (TPR) profiles of the catalysts were determined using a Micromeritics Autochem 2920 equipped with a thermal conductivity detector (TCD). These catalysts were first heated from ambient temperature to 550 $^\circ\text{C}$ at 10 $^\circ\text{C}/\text{min}$ under a 5% O $_2$ /He mixture flow at 50 mL/min for pre-treatment and then exposed to a flowing gas composed of H $_2$ and Ar ($v/v = 1:9$) at 50 mL/min and were heated from room temperature to 700 $^\circ\text{C}$ at a heating rate of 10 $^\circ\text{C}/\text{min}$.

The morphologies of the spent catalyst were analyzed using a JEOL 2100F transmission electron microscope equipped with an energy-dispersive X-ray spectroscopy (EDS-INCA system from Oxford Instrument).

The thermogravimetric analysis (TGA) of the fresh/spent catalysts was conducted on a thermogravimetric analysis unit (Perkin Elmer Pyris 1 TGA unit). The TGA measurements were performed at 10 $^\circ\text{C}/\text{min}$ over a temperature range of 50 $^\circ\text{C}$ to 800 $^\circ\text{C}$ under a constant flow of air of 20 mL/min.

The ICP-AES analysis of the selective fresh and spent catalysts was performed by a certified analytical lab—Lakehead University Instrumentation Lab—following its well-established protocol.

3.4. Catalytic Tests

The hydrogenolysis of glycerol was carried out in a bench scale continuous down-flow tubular reactor (Inconel 316 tubing, 9.55 mm OD, 6.34 mm ID and 600 mm length) heated with an electric furnace. Typically, around 2.0 g of the catalyst was loaded in the constant temperature section of the reactor and supported on a porous Inconel metal disc (pore size: 100 μm) and some quartz wool. Prior to each run, the catalyst was reduced in situ in flowing H $_2$ (100 cm 3 /min) at 300 $^\circ\text{C}$ for 3 h at atmospheric pressure. The feed—a 10 wt% aqueous solution of glycerol (unless otherwise mentioned)—was pumped using a HPLC pump (Eldex) at a predetermined flow rate into the reactor. This translates to a corresponding WHSV, which is the mass of the glycerol per mass of catalyst per hour. All of the experiments are performed at a desired temperature and pressure (controlled by a temperature controller and a back-pressure controller, respectively) along with co-feeding of H $_2$ gas. The liquid and gas products were cooled and collected in a gas-liquid separator immersed in an ice-water trap.

3.5. Product Analysis

All the liquid components in the reaction mixture were analyzed by GC-MS on a Varian 1200 Quadrupole MS (EI) and Varian CP-3800 GC with VF-5 MS column (5% phenyl/95% dimethyl-polysiloxane, 30 m \times 0.25 mm \times 0.25 μm) using helium as the carrier gas at a flow rate of 0.5 mL/s. The oven temperature was maintained at 70 $^\circ\text{C}$ for 1 min and then increased to 290 $^\circ\text{C}$ at 40 $^\circ\text{C}/\text{min}$. Injector and detector temperature were 300 $^\circ\text{C}$. The components were identified by the NIST 98 MS library. Quantification of the chemical composition was performed on a GC-FID (Shimadzu-2010), from Shimadzu Scientific Instruments (Guelph, ON, Canada), calibrated with 1,2-PDO (99.9%), ethylene glycol (99.9%), and acetol (99.8%). Dimethyl sulfoxide (DMSO) was used as the internal standard. The GC-FID analysis was carried out using the similar separation conditions as mentioned above for the GC-MS analysis. The gas samples were analyzed by a GC-TCD (Agilent 3000 Micro-GC).

The reported yield and conversion are values after 4 h on-stream unless otherwise specified. Herewith, the product yield, glycerol conversion, and product selectivity are defined as follows:

$$\text{Yield}(\%) = \frac{\text{Moles of the product formed}}{\text{Initial mole of glycerol}} \times 100 \quad (1)$$

$$\text{Conversion}(\%) = \frac{\text{Initial mole of glycerol} - \text{Final mole of glycerol}}{\text{Initial mole of glycerol}} \times 100 \quad (2)$$

$$\text{Selectivity}(\%) = \frac{\text{Moles of the product formed}}{\text{Initial mole of glycerol} - \text{Final mole of glycerol}} \times 100 = \text{Yield} / \text{Conversion} \quad (3)$$

4. Conclusions

The addition of B₂O₃ to Cu/Al₂O₃ catalysts enhanced the catalytic activity for the hydrogenolysis of glycerol to 1,2-PDO. Among all catalysts prepared and tested, 5Cu-1B/Al₂O₃ demonstrated the best catalytic performance with 98 ± 2% glycerol conversion and 98 ± 2% 1,2-PDO selectivity in hydrogenolysis of 10 wt% aqueous solution of glycerol at the optimum conditions (250 °C, 6 MPa H₂ pressure, and 0.1 h⁻¹ WHSV). Process parameters, such as temperature, hydrogen pressure, and liquid hourly space velocity, significantly influenced the catalytic activity for the glycerol hydrogenolysis reaction. The use of different grades of glycerol, including pharmaceutical-grade glycerol, technical-grade glycerol, and crude glycerol (glycerol purity varying from 54.7 to 99.9%) showed that the presence of impurities could reduce the glycerol conversion and 1,2-PDO selectivity. The long-term stability test demonstrated that the 5Cu-1B/Al₂O₃ catalyst could be used up to 60 h without any appreciable change in activity. Destruction of the support structure, sintering of Cu metal, and coke deposition on the catalyst might be the main factors that deactivated the catalyst after 60 h on stream. The promoting effects of boron for the activities of Cu/Al₂O₃ catalysts might be attributed to the strong interaction between Cu and B species that helped retard the aggregation of Cu particles during calcination, reduction, and reaction, as evidenced by H₂-TPR profiles. In addition, as evidenced by the NH₃-TPD profiles of the catalysts, the addition of B₂O₃ enhanced the acidity of the Cu/Al₂O₃ catalysts, which would also play a role in the enhancement of catalytic activities of the catalysts.

Acknowledgments: The authors wish to acknowledge the financial support provided by Natural Science and Engineering Research Council of Canada (NSERC) through the Discovery Grant and Industrial Research Chair for Xu, as well as from Mitacs through the Accelerate program. We are also grateful to Yasuo Ohtsuka for his invaluable suggestions on some aspects of this research.

Author Contributions: Hengfu Shui and Chunbao (Charles) Xu conceived and designed the experiments; Malaya R. Nanda and Zhongshun Yuan performed the experiments and analyzed the data; and Malaya R. Nanda wrote the paper.

Conflicts of Interest: The authors declare no conflict of interest.

References

1. Maris, E.; Ketchie, W.; Murayama, M.; Davis, R. Glycerol hydrogenolysis on carbon-supported PtRu and AuRu bimetallic catalysts. *J. Catal.* **2007**, *251*, 281–294. [[CrossRef](#)]
2. Yuan, Z.; Wang, J.; Wang, L.; Xie, W.; Chen, P.; Hou, Z.; Zheng, X. Biodiesel derived glycerol hydrogenolysis to 1,2-propanediol on Cu/MgO catalysts. *Bioresour. Technol.* **2010**, *101*, 7099–7103. [[CrossRef](#)] [[PubMed](#)]
3. Nanda, M.R.; Yuan, Z.; Qin, W.; Ghaziaskar, H.S.; Poirier, M.-A.; Xu, C. A new continuous-flow process for catalytic conversion of glycerol to oxygenated fuel additive: Catalyst screening. *Appl. Energy* **2014**, *123*, 75–81. [[CrossRef](#)]
4. Nanda, M.R.; Yuan, Z.; Qin, W.; Ghaziaskar, H.S.; Poirier, M.-A.; Xu, C. Thermodynamic and kinetic studies of a catalytic process to convert glycerol into solketal as an oxygenated fuel additive. *Fuel* **2014**, *117*, 470–477. [[CrossRef](#)]
5. Behr, A.; Eilting, J.; Irawadi, K.; Leschinski, J.; Lindner, F. Improved utilisation of renewable resources: New important derivatives of glycerol. *Green Chem.* **2008**, *10*, 13–30. [[CrossRef](#)]
6. Ma, L.; He, D.; Li, Z. Promoting effect of rhenium on catalytic performance of Ru catalysts in hydrogenolysis of glycerol to propanediol. *Catal. Commun.* **2008**, *9*, 2489–2495. [[CrossRef](#)]
7. Feng, J.; Fu, H.; Wang, J.; Li, R.; Chen, H.; Li, X. Hydrogenolysis of glycerol to glycols over ruthenium catalysts: Effect of support and catalyst reduction temperature. *Catal. Commun.* **2008**, *9*, 1458–1464. [[CrossRef](#)]
8. Sharma, R.V.; Kumar, P.; Dalai, A.K. Selective hydrogenolysis of glycerol to propylene glycol by using Cu:Zn:Cr:Zr mixed metal oxides catalyst. *Appl. Catal. A Gen.* **2014**, *477*, 147–156. [[CrossRef](#)]

9. Yuan, Z.; Wang, L.; Wang, J.; Xia, S.; Chen, P.; Hou, Z.; Zheng, X. Hydrogenolysis of glycerol over homogeneously dispersed copper on solid base catalysts. *Appl. Catal. B Environ.* **2011**, *101*, 431–440. [[CrossRef](#)]
10. Xia, S.; Yuan, Z.; Wang, L.; Chen, P.; Hou, Z. Hydrogenolysis of glycerol on bimetallic Pd-Cu/solid-base catalysts prepared via layered double hydroxides precursors. *Appl. Catal. A Gen.* **2011**, *403*, 173–182. [[CrossRef](#)]
11. Atia, H.; Armbruster, U.; Martin, A. Dehydration of glycerol in gas phase using heteropolyacid catalysts as active compounds. *J. Catal.* **2008**, *258*, 71–82. [[CrossRef](#)]
12. Auttanat, T.; Jongpatiwut, S.; Rirksomboon, T. Dehydroxylation of glycerol to propylene glycol over Cu-ZnO/Al₂O₃ Catalyst: Effect of feed purity. *World Acad. Sci. Technol.* **2012**, *6*, 400–403.
13. Barbelli, M.L.; Santori, G.F.; Nichio, N.N. Aqueous phase hydrogenolysis of glycerol to bio-propylene glycol over Pt-Sn catalysts. *Bioresour. Technol.* **2012**, *111*, 500–503. [[CrossRef](#)] [[PubMed](#)]
14. Dasari, M.; Kiatsimkul, P.-P.; Sutterlin, W.R.; Suppes, G.J. Low-pressure hydrogenolysis of glycerol to propylene glycol. *Appl. Catal. A Gen.* **2005**, *281*, 225–231. [[CrossRef](#)]
15. Deng, C.; Duan, X.; Zhou, J.; Chen, D.; Zhou, X.; Yuan, W. Size effects of Pt-Re bimetallic catalysts for glycerol hydrogenolysis. *Catal. Today* **2014**, *234*, 208–214. [[CrossRef](#)]
16. D'Hondt, E.; Van de Vyver, S.; Sels, B.F.; Jacobs, P. Catalytic glycerol conversion into 1,2-propanediol in absence of added hydrogen. *Chem. Commun.* **2008**, 6011–6012. [[CrossRef](#)] [[PubMed](#)]
17. Kim, N.D.; Park, J.R.; Park, D.S.; Kwak, B.K.; Yi, J. Promoter effect of Pd in CuCr₂O₄ catalysts on the hydrogenolysis of glycerol to 1,2-propanediol. *Green Chem.* **2012**, *14*, 2638–2646. [[CrossRef](#)]
18. Balaraju, M.; Rekha, V.; Prasad, P.S.S.; Devi, B.L.A.P.; Prasad, R.B.N.; Lingaiah, N. Influence of solid acids as co-catalysts on glycerol hydrogenolysis to propylene glycol over Ru/C catalysts. *Appl. Catal. A Gen.* **2009**, *354*, 82–87. [[CrossRef](#)]
19. Zhou, C.-H.C.; Beltramini, J.N.; Fan, Y.-X.; Lu, G.Q.M. Chemoselective catalytic conversion of glycerol as a biorenewable source to valuable commodity chemicals. *Chem. Soc. Rev.* **2008**, *37*, 527–549. [[CrossRef](#)] [[PubMed](#)]
20. Vasiliadou, E.S.; Eggenhuisen, T.M.; Munnik, P.; de Jongh, P.E.; de Jong, K.P.; Lemonidou, A.A. Synthesis and performance of highly dispersed Cu/SiO₂ catalysts for the hydrogenolysis of glycerol. *Appl. Catal. B Environ.* **2014**, *145*, 108–119. [[CrossRef](#)]
21. Gandarias, I.; Arias, P.L.; Requies, J.; El Doukkali, M.; Güemez, M.B. Liquid-phase glycerol hydrogenolysis to 1,2-propanediol under nitrogen pressure using 2-propanol as hydrogen source. *J. Catal.* **2011**, *282*, 237–247. [[CrossRef](#)]
22. Xiao, Z.; Wang, X.; Xiu, J.; Wang, Y.; Williams, C.T.; Liang, C. Synergetic effect between Cu⁰ and Cu⁺ in the Cu-Cr catalysts for hydrogenolysis of glycerol. *Catal. Today* **2014**, *234*, 200–207. [[CrossRef](#)]
23. Panyad, S.; Jongpatiwut, S.; Sreethawong, T.; Rirksomboon, T.; Osuwan, S. Catalytic dehydroxylation of glycerol to propylene glycol over Cu-ZnO/Al₂O₃ catalysts: Effects of catalyst preparation and deactivation. *Catal. Today* **2011**, *174*, 59–64. [[CrossRef](#)]
24. Chaminand, J.; Djakovitch, L.; Gallezot, P.; Marion, P.; Pinel, C.; Rosier, C. Glycerol hydrogenolysis on heterogeneous catalysts. *Green Chem.* **2004**, *6*, 359–361. [[CrossRef](#)]
25. Miyazawa, T.; Kusunoki, Y.; Kunimori, K.; Tomishige, K. Glycerol conversion in the aqueous solution under hydrogen over Ru/C + an ion-exchange resin and its reaction mechanism. *J. Catal.* **2006**, *240*, 213–221. [[CrossRef](#)]
26. Schmidt, S.R.; Tanielyan, S.K.; Marin, N.; Alvez, G.; Augustine, R.L. Selective conversion of glycerol to propylene glycol over fixed bed Raney[®] Cu catalysts. *Top. Catal.* **2010**, *53*, 1214–1216. [[CrossRef](#)]
27. Zhu, S.; Gao, X.; Zhu, Y.; Zhu, Y.; Zheng, H.; Li, Y. Promoting effect of boron oxide on Cu/SiO₂ catalyst for glycerol hydrogenolysis to 1,2-propanediol. *J. Catal.* **2013**, *303*, 70–79. [[CrossRef](#)]
28. Mizugaki, T.; Arundhati, R.; Mitsudome, T.; Jitsukawa, K.; Kaneda, K. Selective hydrogenolysis of glycerol to 1,3-propanediol catalyzed by Pt nanoparticles-AlO_x/WO₃. *Chem. Lett.* **2013**, *42*, 729–731. [[CrossRef](#)]
29. Furikado, I.; Miyazawa, T.; Koso, S.; Shimao, A.; Kunimori, K.; Tomishige, K. Catalytic performance of Rh/SiO₂ in glycerol reaction under hydrogen. *Green Chem.* **2007**, *9*, 582–588. [[CrossRef](#)]
30. Huang, Z.; Liu, H.; Cui, F.; Zuo, J.; Chen, J.; Xia, C. Effects of the precipitation agents and rare earth additives on the structure and catalytic performance in glycerol hydrogenolysis of Cu/SiO₂ catalysts prepared by precipitation-gel method. *Catal. Today* **2014**, *234*, 223–232. [[CrossRef](#)]

31. Huang, Z.; Cui, F.; Xue, J.; Zuo, J.; Chen, J.; Xia, C. Cu/SiO₂ catalysts prepared by hom- and heterogeneous deposition–precipitation methods: Texture, structure, and catalytic performance in the hydrogenolysis of glycerol to 1,2-propanediol. *Catal. Today* **2012**, *183*, 42–51. [[CrossRef](#)]
32. Wang, S.; Liu, H. Selective hydrogenolysis of glycerol to propylene glycol on Cu-ZnO catalysts. *Catal. Lett.* **2007**, *117*, 62–67. [[CrossRef](#)]
33. Bienholz, A.; Schwab, F.; Claus, P. Hydrogenolysis of glycerol over a highly active CuO/ZnO catalyst prepared by an oxalate gel method: Influence of solvent and reaction temperature on catalyst deactivation. *Green Chem.* **2010**, *12*, 290–295. [[CrossRef](#)]
34. Hao, S.-L.; Peng, W.-C.; Zhao, N.; Xiao, F.-K.; Wei, W.; Sun, Y.-H. Hydrogenolysis of glycerol to 1,2-propanediol catalyzed by Cu-H₄SiW₁₂O₄₀/Al₂O₃ in liquid phase. *J. Chem. Technol. Biotechnol.* **2010**, *85*, 1499–1503. [[CrossRef](#)]
35. Vila, F.; López Granados, M.; Ojeda, M.; Fierro, J.L.G.; Mariscal, R. Glycerol hydrogenolysis to 1,2-propanediol with Cu/ γ -Al₂O₃: Effect of the activation process. *Catal. Today* **2012**, *187*, 122–128. [[CrossRef](#)]
36. Niu, L.; Wei, R.; Yang, H.; Li, X.; Jiang, F.; Xiao, G. Hydrogenolysis of glycerol to propanediols over Cu-MgO/USY catalyst. *Chin. J. Catal.* **2013**, *34*, 2230–2235. [[CrossRef](#)]
37. Xia, S.; Yuan, Z.; Wang, L.; Chen, P.; Hou, Z. Catalytic production of 1,2-propanediol from glycerol in bio-ethanol solvent. *Bioresour. Technol.* **2012**, *104*, 814–817. [[CrossRef](#)] [[PubMed](#)]
38. Zheng, J.; Xia, Z.; Li, J.; Lai, W.; Yi, X.; Chen, B.; Fang, W.; Wan, H. Promoting effect of boron with high loading on Ni-based catalyst for hydrogenation of thiophene-containing ethylbenzene. *Catal. Commun.* **2012**, *21*, 18–21. [[CrossRef](#)]
39. Ma, L.; He, D. Influence of catalyst pretreatment on catalytic properties and performances of Ru-Re/SiO₂ in glycerol hydrogenolysis to propanediols. *Catal. Today* **2010**, *149*, 148–156. [[CrossRef](#)]
40. Perosa, A.; Tundo, P. Selective Hydrogenolysis of Glycerol with Raney Nickel. *Ind. Eng. Chem. Res.* **2005**, *44*, 8535–8537. [[CrossRef](#)]
41. Gandarias, I.; Fernández, S.G.; El Doukkali, M.; Requies, J.; Arias, P.L. Physicochemical Study of Glycerol Hydrogenolysis Over a Ni-Cu/Al₂O₃ Catalyst Using Formic Acid as the Hydrogen Source. *Top. Catal.* **2013**, *56*, 995–1007. [[CrossRef](#)]
42. Lewandowski, M.; Sarbak, Z. The effect of boron addition on hydrodesulfurization and hydrodenitrogenation activity of NiMo/Al₂O₃ catalysts. *Fuel* **2000**, *79*, 487–495. [[CrossRef](#)]
43. Zhou, J.; Guo, L.; Guo, X.; Mao, J.; Zhang, S. Selective hydrogenolysis of glycerol to propanediols on supported Cu-containing bimetallic catalysts. *Green Chem.* **2010**, *12*, 1835–1843. [[CrossRef](#)]
44. Guerreiro, E.D.; Gorriz, O.F.; Rivarola, J.B.; Arrúa, L.A. Characterization of Cu/SiO₂ catalysts prepared by ion exchange for methanol dehydrogenation. *Appl. Catal. A Gen.* **1997**, *165*, 259–271. [[CrossRef](#)]
45. Tan, K.F.; Chang, J.; Borgna, A.; Saeys, M. Effect of boron promotion on the stability of cobalt Fischer-Tropsch catalysts. *J. Catal.* **2011**, *280*, 50–59.
46. Yin, A.; Qu, J.; Guo, X.; Dai, W.-L.; Fan, K. The influence of B-doping on the catalytic performance of Cu/HMS catalyst for the hydrogenation of dimethyl oxalate. *Appl. Catal. A Gen.* **2011**, *400*, 39–47. [[CrossRef](#)]
47. He, Z.; Lin, H.; He, P.; Yuan, Y. Effect of boric oxide doping on the stability and activity of a Cu-SiO₂ catalyst for vapor-phase hydrogenation of dimethyl oxalate to ethylene glycol. *J. Catal.* **2011**, *277*, 54–63. [[CrossRef](#)]
48. Zhao, S.; Yue, H.; Zhao, Y.; Wang, B.; Geng, Y.; Lv, J.; Wang, S.; Gong, J.; Ma, X. Chemoselective synthesis of ethanol via hydrogenation of dimethyl oxalate on Cu/SiO₂: Enhanced stability with boron dopant. *J. Catal.* **2013**, *297*, 142–150. [[CrossRef](#)]
49. Martin, A.; Armbruster, U.; Gandarias, I.; Arias, P.L. Glycerol hydrogenolysis into propanediols using in situ generated hydrogen—A critical review. *Eur. J. Lipid Sci. Technol.* **2013**, *115*, 9–27. [[CrossRef](#)]
50. Vasiliadou, E.S.; Lemonidou, A. Glycerol transformation to value added C₃ diols: Reaction mechanism, kinetic, and engineering aspects. *Wiley Interdiscip. Rev. Energy Environ.* **2014**, *4*, 486–520. [[CrossRef](#)]
51. Zhou, J.; Zhang, J.; Guo, X.; Mao, J.; Zhang, S. Ag/Al₂O₃ for glycerol hydrogenolysis to 1,2-propanediol: Activity, selectivity and deactivation. *Green Chem.* **2012**, *14*, 156–163. [[CrossRef](#)]

